

3D nerve proximity mapping of the medial branch of lumbar dorsal ramus: An anatomical study

John Tran, PhD^{a,b,c,*}, Arden Lawson^{b,c}, Nicole Billias^{b,c}, Eldon Loh^{b,c}

^a Division of Anatomy, Department of Surgery, University of Toronto, Toronto, Ontario, M5S 1A8, Canada

^b Department of Physical Medicine and Rehabilitation, Western University, Schulich School of Medicine and Dentistry, London, Ontario, N6C 0A7, Canada

^c Parkwood Institute Research, Lawson Health Research Institute, London, Ontario, N6C 2R5, Canada

ABSTRACT

Objective: Lumbar medial branch (MB) radiofrequency ablation is a common intervention to treat facetogenic low back pain. Consensus among spine pain interventionalists is that the cannula tip should be placed adjacent to the periosteum of the lateral neck of the superior articular process (SAP) to ensure maximum contact with the MB. The spatial relationship of the nerve to the periosteum of the lateral neck of the SAP has not been quantified in 3D. The objectives of the current study were to: 1) use 3D modelling technology to quantify the location along the lateral neck of the SAP where the MB is in direct contact with the periosteum; and 2) identify target site(s) to optimize lumbar MB denervation.

Design: Seventy lumbar dorsal rami in 14 formalin-embalmed specimens were dissected, digitized, and modeled in 3D. The 3D positional data of the MB were used to generate a novel nerve proximity map which provided a method to quantify and visualize the 3D course of the MB in relation to the periosteum of the lateral neck of SAP. The percent of the lateral neck of SAP in contact with the MB was quantified and consistent target site(s) identified.

Results: There was variability in the percentage of the lateral neck of SAP in contact with the MB. The mean percentage of the lateral neck of SAP in contact with the MB for the L1-L5 levels ranged between $57.39 \pm 10.72\%$ (for L1) to $81.54 \pm 10.48\%$ (for L5). The nerve proximity map showed consistent course of the MB along the posterior portion of the lateral neck of SAP and at a novel target site distal to the mamillo-accessory notch (i.e. sub-mammillary landmark).

Conclusion: The percent of the lateral neck that was in contact with the MB was quantified and visualized using a novel nerve proximity mapping methodology which may be used to inform cannula tip depth placement. Further, the nerve proximity maps were used to identify an alternative landmark to extend the length of the MB captured. The proposed sub-mammillary landmark may be a viable target site pending future anatomical and clinical investigations.

1. Introduction

Chronic facetogenic low back pain is commonly treated with lumbar medial branch (MB) radiofrequency ablation (RFA) [1]. It is believed that capturing a greater length of the MB correlates with a longer duration of pain relief [2–4]. Therefore, there has been interest in optimization of parallel techniques using conventional electrodes [5–9], and use of perpendicular approaches with expanded lesions [10,11], to maximize nerve capture and prolong treatment duration.

Lumbar RFA traditionally targets the MB along the middle two quarters of the lateral neck of the superior articular process (SAP) using a parallel approach [2,4,5]. More recent anatomical studies have proposed the posterior portion of the lateral neck as a viable target site [6,8] with early clinical evidence supporting its feasibility and effectiveness [9]. The current consensus among spine pain interventionalists is that the cannula tip should be placed adjacent to the periosteum of the lateral neck of the SAP to ensure maximum contact with the MB to produce a

high-quality denervation. This rationale is based on the anatomical understanding that the MB courses along the periosteum of the lateral neck of the SAP. However, although previous studies have investigated the anatomy of the MB [5,6], the spatial relationship of the nerve to the lateral neck of the SAP has not been quantified in 3D. As a result, the portion of the lateral neck where the MB is in contact with the periosteum is not clearly defined, which is important to determine optimal cannula tip positioning to maximize the length of the nerve captured.

With advances in high-fidelity 3D modelling technology, the spatial relationships of nerve branches and anatomical landmarks can be reconstructed from cadaveric specimens [12,13]. The application of this technology to document the 3D positional data of the MB enables the visualization and quantification of their relationship to the lateral neck of the SAP to optimize lumbar RFA. Therefore, the objectives of the current study were to: 1) use 3D modelling technology to quantify the location along the lateral neck of the SAP where the MB is in direct contact with the periosteum; and 2) identify target site(s) to optimize

* Corresponding author. Division of Anatomy, Department of Surgery, University of Toronto, Toronto, Ontario, Canada.

E-mail addresses: johnjt.tran@utoronto.ca (J. Tran), arden.lawson@sjhc.london.on.ca (A. Lawson), nicole.billias@sjhc.london.on.ca (N. Billias), eldon.loh@sjhc.london.on.ca (E. Loh).

<https://doi.org/10.1016/j.inpm.2024.100414>

Received 12 April 2024; Received in revised form 8 May 2024; Accepted 10 May 2024

Available online 15 May 2024

2772-5944/© 2024 The Authors. Published by Elsevier Inc. on behalf of International Pain & Spine Intervention Society. This is an open access article under the CC BY-NC-ND license (<http://creativecommons.org/licenses/by-nc-nd/4.0/>).

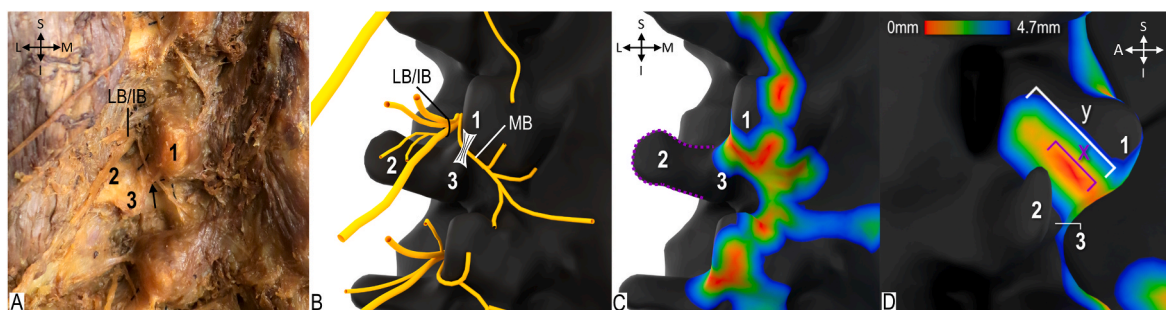


Fig. 1. Methodology. A. Cadaveric dissection of lumbar dorsal rami, left oblique view. B. High-fidelity 3D model of lumbar dorsal rami and lumbosacral spine, left oblique view. C. Nerve proximity mapping of the position of medial branch (MB) relative to the periosteum, left oblique view. D. Distance measurements of the lateral neck of the superior articular process (Y) and portion in contact with medial branch (X), lateral view. 1 indicates mammillary process; 2, transverse process; 3, accessory process; LB/IB, lateral and intermediate branches; Dashed purple curve, outline of transverse process; Black arrow, mamillo-accessory ligament. (For interpretation of the references to color in this figure legend, the reader is referred to the Web version of this article.)

lumbar MB denervation.

2. Methods

2.1. Cadaveric specimens

Seventy lumbar dorsal rami in 14 formalin-embalmed specimens (mean age of 75.4 ± 13.8 years; 6 females/8 males) were dissected, digitized, and modeled in 3D. No other demographic data was available. The University of Toronto Health Sciences Research Ethics Board approved this cadaveric study (protocol #27210).

2.2. Dissection, digitization, and 3D modeling protocol

The skin, fascia and superficial back muscles of each specimen were excised to expose the erector spinae muscle group. Next, the erector spinae were dissected away by carefully removing muscle fiber bundles to expose the LB and IB of the lumbar dorsal rami (L1-L5) as *in situ*. The nerve branches were meticulously traced proximally towards the intervertebral foramen to locate the origin of the MB of the lumbar dorsal ramus. The MB was then dissected, and its articular branches traced to their termination in the lumbar facet joint capsules (Fig. 1A).

Following dissection, the branches of the lumbar dorsal rami and bony surfaces were digitized using a Microscribe G2X Digitizer (Immersion Corporation, San Jose, CA, USA; accuracy ± 0.23 mm). The Microscribe digitization method enables the capture of 3D positional data as Cartesian coordinates [14,15]. Nerve thickness was also documented by digitizing the diameter of each branch at 1 cm intervals which was used for volumetric reconstruction. Next, to generate a high-fidelity reconstruction of the lumbosacral spine, the vertebral column and sacrum were skeletonized leaving only the capsule of the facet joints and vertebral ligaments intact. Each skeletonized specimen was then scanned using a Faro Laser ScanArm (FARO Technologies, Lake Mary, Florida, USA; accuracy ± 35 μ m). The digitized nerves and bony surfaces, along with the high-resolution surface scan, were imported into Blender3D (Blender Foundation, Amsterdam, NL) and aligned to generate high-fidelity 3D models as *in situ* (Fig. 1B). The branches of the lumbar dorsal rami were volumetrically reconstructed as cylinder tubes with diameters matching the digitized thickness of each nerve.

2.3. Medial branch nerve proximity mapping protocol

The 3D positional data of the MB of L1-L5 dorsal rami were used to generate a nerve proximity map. The positional data of the nerve was mapped onto the high-resolution surface scan of the lumbosacral spine using Blender3D and custom developed plugins (Fig. 1C). The nerve proximity map provides a quantified method to visualize the 3D course of the MB in relationship to the periosteum of the lateral neck of SAP.

Each surface point on the high-resolution surface scan was computationally assigned a gradient color based on calculated minimal distance between each point and the MB. Points that were in contact with the nerve (i.e., 0 mm away) were colored red; points that were 4.7 mm away were assigned blue, and >4.7 mm away were black. The 4.7 mm distance was selected as the limit for analysis based on the lesion diameter generated by a conventional 16G cannula with a 10 mm tip at 80 °C for 2 min ($9.4\text{mm}/2 = 4.7$ mm) [16]. Therefore, the nerve proximity map generated, with this value, is a visual representation of the range of positions a conventional 16G needle can be placed to generate a lesion that can theoretically reach the MB.

2.4. Distance measurement protocol

The nerve proximity map was used to visualize and describe, using percentages, the location along the lateral neck of SAP where the MB was in direct contact with the periosteum (i.e., 0 mm away). To accomplish this, images of the high-fidelity 3D models, with nerve proximity mapping, were rendered using Blender3D to match direct lateral radiographs. The images were imported into ImageJ (a free open-source software) for distance measurements. Two distances were measured to calculate the percent of lateral neck of SAP in direct contact with the MB (Fig. 1D). The first was the entire length of the lateral neck of SAP (y, Fig. 1D) and the second was the portion, beginning at the posterior margin of the lateral neck of SAP, that was colored red (x, Fig. 1D) which represented the area in direct contact with the MB. The percentage was calculated ($x/y \times 100$) and was performed at the L1-L5 levels. As such, a percentage of 25 % would describe contact of the MB with the periosteum from the posterior margin up to the posterior quarter of the lateral neck of the SAP. Percentages greater than 50 % would describe contact of the MB from the posterior margin into the anterior half of the lateral neck of SAP. Clinically, the expressed percentage would correlate with the depth that a needle could be advanced along the periosteum of the lateral neck of SAP, as visualized on a lateral radiograph, if a “parallel” approach is used.

2.5. Data analysis

The mean percentages of the lateral neck of SAP in direct contact with the MB were calculated and compared between the L1-L5 levels. The normality of the dataset was assessed using the Shapiro-Wilk test. A one-way ANOVA was performed to determine if mean differences between the L1-L5 levels were statistically significant with subsequent post hoc Tukey HSD analysis.

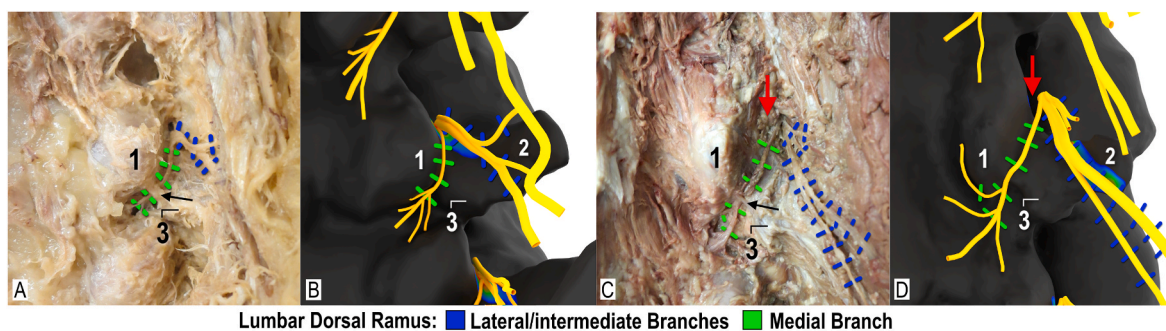


Fig. 2. Dissection and high-fidelity modelling of lumbar dorsal rami, right oblique view. A and B. Dissection and corresponding 3D model showing medial branch following the entire contour of the lateral neck of the superior articular process. C and D. Dissection and corresponding 3D model showing medial branch originating more laterally and coursing partially along the lateral neck. Red arrow indicates space between the lateral neck of the superior articular process and medial branch; Black arrow, mamillo-accessory ligament; 1, mammillary process; 2, transverse process; 3, accessory process. (For interpretation of the references to color in this figure legend, the reader is referred to the Web version of this article.)

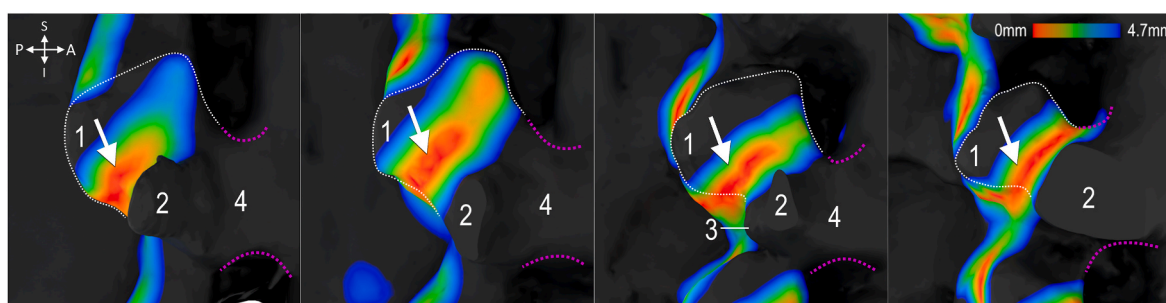


Fig. 3. Variation in the percentage of lateral neck of superior articular process in contact with medial branch, lateral views. 1 indicates mammillary process; 2, transverse process; 3, accessory process; 4, pedicle; Dashed white line, outline of superior articular process; Dashed pink line, superior and inferior contour of pedicle; White arrow, posterior portion of lateral neck in contact with medial branch in all specimens. (For interpretation of the references to color in this figure legend, the reader is referred to the Web version of this article.)

Table 1
Summary of the percent (%) of the lateral neck in contact with medial branch.

	SP1	SP2	SP3	SP4	SP5	SP6	SP7	SP8	SP9	SP10	SP11	SP12	SP13	SP14	Mean ± SD
L1	47.36	57.99	61.00	47.21	69.43	66.73	65.87	50.18	42.05	55.8	64.77	42.94	77.63	54.42	57.39 ± 10.72
L2	54.91	60.57	63.4	53.55	62.41	87.57	43.52	35.86	52.17	81.98	63.07	45.67	72.07	62.27	59.93 ± 14.17
L3	53.83	72.91	76.53	70.96	69.22	89.84	64.00	69.82	48.25	44.74	85.42	65.45	65.63	61.82	67.03 ± 12.64
L4	77.85	71.25	70.44	74.84	48.97	67.17	84.48	60.15	87.28	98.32	84.72	67.19	97.66	54.25	74.61 ± 14.90
L5	79.12	89.44	91.59	75.69	87.50	85.86	84.29	88.86	75.71	56.84	78.02	72.16	100.00	76.56	81.54 ± 10.48

3. Results

3.1. Course of the medial branch

In total 70 lumbar MBs were dissected, digitized and modeled in 3D (Fig. 2). Distally, the MB consistently passed through the mamillo-accessory notch deep to the corresponding ligament in all specimens (Fig. 2A). However, the origin of the MB varied in position. The nerve was found to branch from the lumbar dorsal ramus either more medially or more laterally. If branching medially, the MB followed the contour of the entire lateral neck of the SAP (Fig. 2A and B). Alternatively, if the MB originated from the lumbar dorsal ramus more laterally, it travelled through adipose tissue prior to contacting the periosteum of the lateral neck (Fig. 2C and D). This variation is reflected in the percentage of the lateral neck of SAP (beginning at the posterior margin) that is in direct contact with the MB (Fig. 3). The posterior portion of the lateral neck, proximal to the posterior margin of the SAP, was found to be in contact with the MB in all specimens (Fig. 3, white arrow). Distal to the posterior margin of the lateral neck of SAP, the MB continued to course in a posteromedial direction. After passing through the mamillo-accessory notch, the MB was found inferior to the mammillary process at which

point the nerve further divided into muscular and articular branches (Fig. 2).

3.2. Quantification of the percent of the lateral neck in contact with the medial branch

The extent to which the MB was in contact with the periosteum was quantified in 70 cases and was variable ranging from 35.86 % to 100.00 % of the lateral neck of SAP (Table 1). The mean percentages of the lateral neck of SAP in contact with the MB for the L1-L5 levels were also variable and ranged between 57.39 ± 10.72 % (for L1) to 81.54 ± 10.48 % (for L5). A Shapiro-Wilk test showed no significant departure from normality, $W(70) = 0.98, p = 0.521$. A subsequent 1-way ANOVA test showed that there was a statistically significant difference in percentage of the lateral neck of SAP in contact with the MB between L1-L5 levels ($F(4,65) = [8.801], p < 0.001$). Post hoc Tukey HSD analysis determined that there were statistically significant differences between:

- L1 vs. L4 ($p < 0.01$), L1 vs. L5 ($p < 0.001$)
- L2 vs. L4 ($p = 0.03$), L2 vs. L5 ($p < 0.001$)
- L3 vs. L5 ($p = 0.02$)

4. Discussion

Optimization of fluoroscopic guided lumbar MB denervation requires a robust understanding of the anatomical relationship of the nerve to bony landmarks. Consensus among spine pain interventionists is that parallel placement of the cannula tip adjacent to the periosteum along the lateral neck of the SAP (i.e., hugging the neck) ensures maximum needle-to-nerve contact and coagulation. In the current study, the position of the MB in relationship to the lateral neck of the SAP was quantified in 3D and analyzed using a novel nerve proximity mapping methodology. Using this methodology, the current study revealed three relevant findings with implications for optimizing lumbar MB denervation. First, the nerve proximity map provides a visual aid that can be used to optimize caudal angulation to maximize needle-to-nerve contact. Second, it provides quantified evidence to analyze the relationship of the MB to the periosteum of the lateral neck to inform target location (e.g. needle depth as seen on a lateral radiograph). Third, it provides a method to identify novel bony targets to potentially increase the length of the MB captured.

4.1. Nerve proximity map as visual aid

Previous anatomical studies have investigated the anatomy of the lumbar dorsal rami using a dissection-based methodology [5,6,17–20]. Early studies published by Bogduk et al., described the detailed course of the MB in relation to the lateral neck of the SAP and mamillo-accessory ligament [17,18]. Subsequent studies investigated 1) the distance between the dorsal ramus bifurcation and the superior border of the root of the transverse process [19]; and 2) the relationship of the MB to fluoroscopic features to inform cannula placement [5,6]. However, no previous studies used a methodology to visualize and quantify the 3D position of the MB in relation to the lateral neck of the SAP with high-fidelity. In the current study, the MB's 3D position was mapped onto the periosteum of the lateral neck of the SAP using a novel nerve proximity mapping methodology. Spine pain interventionists can utilize the nerve proximity map to guide optimal placement of the needle tip adjacent to the MB along the lateral neck of SAP. The nerve proximity map corroborates the previously recommended caudal angulation protocol using the inferior margin of the mammillary process as a reference landmark to achieve parallel and adjacent placement of the needle tip along the MB [6].

Accurate and adjacent placement along the MB is important as thermal energy dissipates with greater distance away from the needle tip [16]. Therefore, heat at the margins of the RFA lesion is lower than at the center of the lesion; maximizing needle-to-nerve contact will ensure higher likelihood of a high-quality thermal coagulation of the targeted nerve. Targeting the needle tip within the red zone on the nerve proximity map would represent the ideal placement to maximize needle-to-nerve contact and ensure more consistent denervation. Although placement of the cannula outside of the red zone may still lead to coagulation, the quality and/or consistency of the denervation may not be optimal as the needle tip would be farther from the MB.

Clinicians should be cognizant that needle gauge and other factors (e.g. temperature) will alter lesion size which may affect clinical success. In the current study, the nerve proximity map was based on a 16G cannula heated to 80 °C for 2 min, which generates a 4.7 mm radius lesion [16]. This type of needle may result in better clinical results as the margin for error is potentially larger due to the greater lesion volume; using a higher gauge needle (i.e. a thinner needle) may require placement with greater precision to capture the MB.

4.2. Medial branch location along periosteum of superior articular process

It is commonly believed that needle placement along the periosteum (i.e. hugging the lateral neck) is important to maximize needle-to-nerve contact. A previous study has recommended targeting the middle two

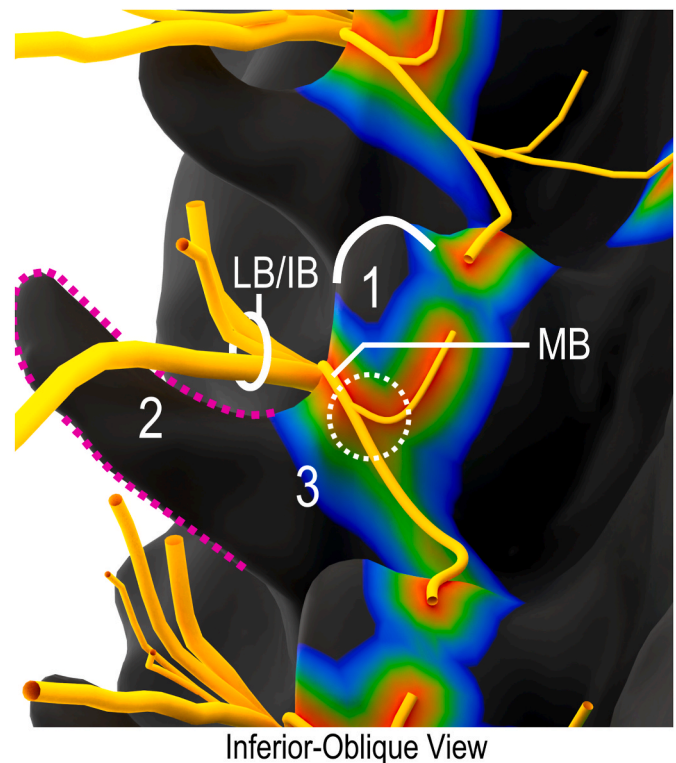


Fig. 4. Novel sub-mammillary landmark identified with medial branch nerve proximity mapping. 1 indicates mammillary process; 2, transverse process; 3, accessory process; Dashed white circle, sub-mammillary landmark; Dashed purple curve, outline of transverse process; LB/IB, lateral and intermediate branches; MB, medial branch; White curve, contour of mammillary process. (For interpretation of the references to color in this figure legend, the reader is referred to the Web version of this article.)

quarters of the lateral neck of SAP (i.e. distal end of needle tip at the anterior quarter) [5]. Based on nerve proximity mapping in the current study, there is support for placement of the needle tip up to a depth of 75 % (anterior quarter) of the lateral neck. However, there are two important considerations with implications on optimal needle depth placement along the lateral neck: (1) variability in the percentage of the MB that is in contact with the periosteum, and (2) risk to other structures with anterior placement.

The percentage of the lateral neck where the MB is in contact with the periosteum (Table 1) ranged from 35.86 % (i.e. from the posterior margin to around the posterior third of the lateral neck) to 100 % (i.e. the entire length of the lateral neck as seen from the lateral view). Although there was variability, the MB in all specimens was consistently in contact with the periosteum at the posterior portion of the lateral neck just proximal to the mamillo-accessory notch (Fig. 3, white arrow). This consistent relationship suggests that the posterior portion of the lateral neck is a more reliable location when trying to target the MB along the periosteum of the SAP. When positioning the cannula along the posterior portion of the lateral neck, a parasagittal approach is usually necessary [7,8]. Conversely, anterior placement along the lateral neck of SAP (up to 75 % depth) requires a more oblique approach to ensure contact with the periosteum [7].

The risk of denervating other neural structures with more anterior placement of the cannula tip has been discussed [21,22] and investigated [23]. Although the risk of inadvertent denervation of other neural structures remains unclear [21–23], it is conceivable that advancing the needle more anterior to capture a greater length of the MB will encroach onto the other branches of the lumbar dorsal ramus. When considering the potential risk of inadvertent denervation (with more anterior placement) and the consistent relationship of the MB along the

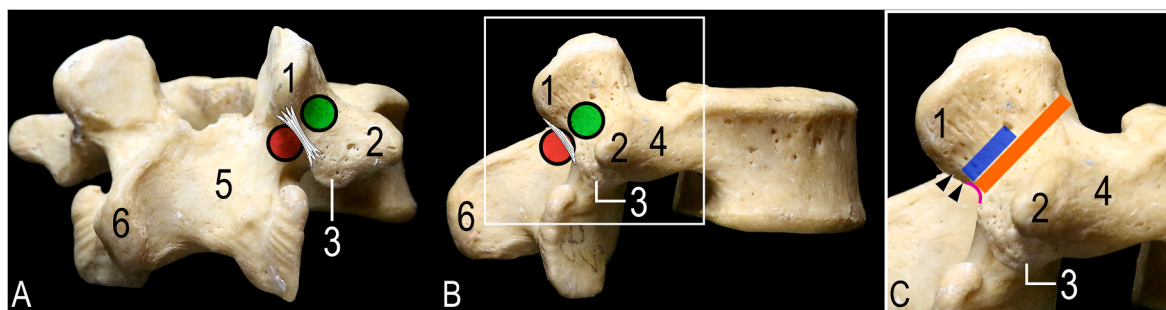


Fig. 5. Schematic diagram demonstrating the proposed sites to target the lumbar medial branch. A. Diagram of proposed target sites on lumbar vertebra relative to mamillo-accessory ligament, oblique view. B. Diagram of proposed target sites relative to mamillo-accessory ligament, lateral view. C. Inset photo of white box in panel B illustrating key anatomical landmarks related to the superior articular process. Orange line indicates the lateral neck of superior articular process; blue line, posterior portion of lateral neck; black arrowheads, posterior margin of the superior articular process; pink curve, mamillo-accessory notch; 1, mammillary process; 2, transverse process; 3, accessory process; 4, pedicle; 5, lamina; 6, spinous process; Green circle, lesion at posterior portion of lateral neck; Red circle, lesion at sub-mammillary landmark. (For interpretation of the references to color in this figure legend, the reader is referred to the Web version of this article.)

periosteum posteriorly, as reported in the current study, the recommendation to target the posterior portion of the lateral neck of SAP may be ideal (e.g. needle depth up to 50 % of lateral neck) [6,8,9].

A perpendicular approach using multi-tined electrodes to target the MB against the periosteum of the lateral neck of the SAP has recently been used clinically [11]. Based on the nerve proximity map in the current study, the consistent relationship of the MB with the periosteum suggests a multi-tined perpendicular approach should also target the posterior half of the lateral neck of the SAP (proximal to mamillo-accessory notch). This target would increase the likelihood of capturing the MB against the periosteum.

4.3. Novel landmark to target the medial branch

Lengthening the portion of the MB captured is commonly believed to prolong pain relief outcomes. Based on the novel nerve proximity map of the MB, locations where the nerve target is consistently associated with the periosteum of the lumbosacral spine were visualized providing insights into where the nerve departs from the bone surface. The MB was consistently found to pass through the mamillo-accessory notch and consequently coursed invariably in two anatomical locations. The first was located proximal/lateral to the mamillo-accessory notch along the posterior half of the lateral neck of the SAP; and the second was distal/medial to the notch and inferior to the mammillary process (i.e., sub-mammillary landmark) deep to the multifidus. The sub-mammillary landmark may represent an alternative target for MB denervation to extend the length of the nerve captured (Figs. 4 and 5). Furthermore, the addition of the sub-mammillary landmark may, in certain instances, overcome anatomical variations and degenerative changes that limit the length of the MB that is captured along the lateral neck when using traditional and/or parasagittal approaches. Clinically, spine pain interventionalists may utilize a dual burn approach to target the lateral neck and sub-mammillary landmarks with parallel and perpendicular techniques, respectively. Future anatomical and clinical research is required to validate the feasibility and safety of the proposed sub-mammillary landmark/technique.

The use of fluoroscopic guided high intensity focused ultrasound (HIFU) as a non-invasive modality for denervating the lumbar MB is an emerging treatment option; early clinical evidence reports similar effectiveness as RFA [24,25]. A HIFU generated focal lesion is likely most effective when targeting the periosteum as it “leverages the high acoustic absorption of bone to create predictable thermal ablation at the bone-tissue interface” [25]. Therefore, nerve proximity mapping in the current study provides a means of identifying optimal target sites for HIFU lesions. Specifically, this study reports a consistent location of the MB at the periosteum of (1) the posterior portion of the lateral neck and (2) the sub-mammillary landmark; these target sites may be ideal for

HIFU focal lesions (Fig. 5). Future research is required to assess the feasibility and effectiveness of HIFU protocols.

4.4. Limitations

The current study is limited by a small sample size which does not encompass all anatomical variations (i.e., interpersonal differences, osteophyte formations, and degenerative changes). However, the number of specimens in the current study is greater than the recommended number for studies with no previous data [26]. The nerve proximity mapping protocol used in the current study was limited to conventional 16G cannula with a 10 mm tip heated to 80 °C for 2 min. Different cannula and lesion configurations may alter the nerve proximity mapping pattern and require separate analysis. As with all anatomical studies, the clinical implications discussed in the current study will require further investigation.

5. Conclusions

In this anatomical study the course of the L1-L5 MBs was documented in 3D relative to the periosteal surface of the lumbosacral spine. The percent of the lateral neck that was in contact with the MB was quantified and visualized using a novel nerve proximity mapping methodology. Variation exists in the percent of the lateral neck that contacts the MB which may be used to inform cannula tip placement. Further, the nerve proximity maps were used to identify an alternative landmark to extend the length of the MB captured. The proposed sub-mammillary landmark may be a viable target site pending future anatomical and clinical investigations.

Declaration of competing interest

The authors declare the following financial interests/personal relationships which may be considered as potential competing interests: Eldon Loh reports financial support was provided by International Pain and Spine Intervention Society. If there are other authors, they declare that they have no known competing financial interests or personal relationships that could have appeared to influence the work reported in this paper.

Acknowledgements

The authors wish to thank the individuals who donated their bodies and tissues for the advancement of education and research. This study was funded by the International Pain and Spine Intervention Society Research Grant awarded to EL & JT.

References

- [1] Manchikanti L, Sanapati MR, Pampati V, et al. Update of utilization patterns of facet joint interventions in managing spinal pain from 2000 to 2018 in the US fee-for-service Medicare population. *Pain Physician* 2020;23:E133–49.
- [2] Bogduk N. Lumbar radiofrequency neurotomy. *Clin J Pain* 2006;22(4):409. <https://doi.org/10.1097/01.ajp.0000182845.55330.9f>.
- [3] Loh JT, Nicol AL, Elashoff D, Ferrante FM. Efficacy of needle placement technique in radiofrequency ablation for treatment of lumbar facet arthropathy. *J Pain Res* 2015;8:687–94. <https://doi.org/10.2147/JPR.S84913>.
- [4] Schneider BJ, Doan L, Maes MK, et al. Standards Division of the Spine Intervention Society. Systematic review of the effectiveness of lumbar medial branch thermal radiofrequency neurotomy, stratified for diagnostic methods and procedural technique. *Pain Med* 2020;21(6):1122–41.
- [5] Lau P, Mercer S, Govind J, et al. The surgical anatomy of lumbar medial branch neurotomy (facet denervation). *Pain Med* 2004;5(3):289–98.
- [6] Tran J, Campisi ES, Agur AMR, Loh E. Anatomical study of the medial branches of the lumbar dorsal rami: implications for image-guided intervention. *Reg Anesth Pain Med* 2022;47:464–74. <https://doi.org/10.1136/rapm-2022-103653>.
- [7] Tran J, Campisi ES, Agur AMR, Loh E. Quantification of needle angles for traditional lumbar medial branch radiofrequency ablation: an osteological study. *Pain Med* 2023;24(5):488–95. <https://doi.org/10.1093/pm/pnac160>.
- [8] Tran J, Campisi ES, Agur AMR, Loh E. Quantification of needle angles for lumbar medial branch denervation targeting the posterior half of the superior articular process: an osteological study. *Pain Med* 2024;25(1):13–9. <https://doi.org/10.1093/pm/pnad105>.
- [9] Tran J, Lawson A, Agur A, Loh E. Parasagittal needle placement approach for lumbar medial branch denervation: a brief technical report. *Reg Anesth Pain Med* 2024. <https://doi.org/10.1136/rapm-2023-105152>. Published Online First: 04 January.
- [10] McCormick ZL, Choi H, Reddy R, et al. Randomized prospective trial of cooled versus traditional radiofrequency ablation of the medial branch nerves for the treatment of lumbar facet joint pain. *Reg Anesth Pain Med* 2019;44(3):389–97. <https://doi.org/10.1136/rapm-2018-000035>.
- [11] Deng G, Smith A, Burnham R. Prospective within subject comparison of fluoroscopically guided lumbosacral facet joint radiofrequency ablation using a multi-tined (trident) versus conventional monopolar cannula. *Pain Physician* 2022; 25(5):391–9.
- [12] Tran J, Peng P, Agur A. Evaluation of suprascapular nerve radiofrequency ablation protocols: 3D cadaveric needle placement study. *Reg Anesth Pain Med* 2019;44: 1021–5.
- [13] Tran J, Peng P, Agur A. Evaluation of nerve capture using classical landmarks for genicular nerve radiofrequency ablation: 3D cadaveric study. *Reg Anesth Pain Med* 2020;45:898–906.
- [14] Loh EY, Agur AM, McKee NH. Intramuscular innervation of the human soleus muscle: a 3D model. *Clin Anat* 2003;16:378–82. <https://doi.org/10.1002/ca.10170>.
- [15] Ravichandiran M, Ravichandiran N, Ravichandiran K, McKee NH, Richardson D, Oliver M, Agur AM. Neuromuscular partitioning in the extensor carpi radialis longus and brevis based on intramuscular nerve distribution patterns: a three-dimensional modeling study. *Clin Anat* 2012;25:366–72. <https://doi.org/10.1002/ca.21246>.
- [16] Cosman ER Jr, Dolensky JR, Hoffman RA. Factors that affect radiofrequency heat lesion size. *Pain Med* 2014;15(12):2020–36. <https://doi.org/10.1111/pme.12566>.
- [17] Bogduk N, Wilson AS, Tynan W. The human lumbar dorsal rami. *J Anat* 1982;134: 383–97.
- [18] Bogduk N. The innervation of the lumbar spine. *Spine* 1983;8:286–93.
- [19] Shuang F, Hou SX, Zhu JL, et al. Clinical anatomy and measurement of the medial branch of the spinal dorsal ramus. *Medicine (Baltim)* 2015;94(52):e2367. <https://doi.org/10.1097/MD.0000000000002367>.
- [20] Saito T, Steinke H, Hammer N, et al. Third primary branch of the posterior ramus of the spinal nerve at the thoracolumbar region: a cadaveric study. *Surg Radiol Anat* 2019;41:951–61. <https://doi.org/10.1007/s00276-019-02258-z>.
- [21] Bryant DG, Dovgan JT, Hunt C, et al. Letter to the editor regarding 'Anatomical study of the medial branches of the lumbar dorsal rami: implications for image-guided intervention'. *Reg Anesth Pain Med* 2023;48:94.
- [22] Tran J, Loh E. Reply to letter to editor regarding 'anatomical study of the medial branches of the lumbar dorsal rami: implications for image guided intervention'. *Reg Anesth Pain Med* 2023;48:95–6.
- [23] Tran J, Campisi E, Roa Agudelo A, et al. High-fidelity 3D modelling of the lumbar dorsal rami. *Intervent Pain Med* 2024;3:100401. <https://doi.org/10.1016/j.inpm.2024.100401>.
- [24] Perez J, Gofeld M, Leblang S, et al. Fluoroscopy-guided high-intensity focused ultrasound neurotomy of the lumbar Zygapophyseal joints: a clinical pilot study. *Pain Med* 2022;23:67–75.
- [25] Gofeld M, Smith KJ, Bhatia A, et al. Fluoroscopy-guided high-intensity focused ultrasound neurotomy of the lumbar zygapophyseal joints: a prospective, open-label study. *Reg Anesth Pain Med* 2024. <https://doi.org/10.1136/rapm-2024-105345>. Published Online First.
- [26] Julious SA. Sample size of 12 per group rule of thumb for a pilot study. *Pharmaceut Stat* 2005;4:287–91. <https://doi.org/10.1002/pst.185>.